RSC Advances

PAPER

View Article Online
View Journal | View Issue

Cite this: *RSC Adv.*, 2019, **9**, 11082

Highly diastereoselective construction of novel dispiropyrrolo[2,1-*a*]isoquinoline derivatives *via* multicomponent 1,3-dipolar cycloaddition of cyclic diketones-based tetrahydroisoquinolinium *N*-ylides†

Sarra Boudriga,*[a] Saoussen Haddad,[a] Moheddine Askri,*[a] Armand Soldera,[b] Michael Knorr,[c] Carsten Strohmann[d] and Christopher Golz[d]

Received 1st December 2018
Accepted 5th March 2019

DOI: 10.1039/c8ra09884k

rsc.li/rsc-advances

In the quest for new heterocyclic scaffolds exhibiting potentially biological activities for medicinal chemistry, a multicomponent 1,3-dipolar cycloaddition reaction of tetrahydroisoquinolinium *N*-ylides, generated *in situ* from cyclic diketones and isoquinoline, and (*E*)-3-arylidene-1-phenyl-pyrrolidine-2,5-diones has been developed. This route provides workable access to dispiropyrrolo[2,1-*a*]isoquinoline-fused pyrrolidine-2,5-diones bearing two adjacent spiro-carbons. An unprecedented regioselectivity was observed in this 1,3-dipolar cycloaddition, leading to the construction of a novel dispirooxindole skeleton. The structure and relative stereochemistry of the spiranic adducts have been confirmed by three X-ray diffraction studies. To reinforce the observed regio- and stereoselectivity of the [3+2] cycloaddition, calculations using the DFT approach at the B3LYP/6-31G(d,p) level were carried out. It was found that this reaction affords the kinetic products.

Introduction

Pyrrolo[2,1-*a*]isoquinolines as structural motifs have drawn considerable interest in the area of synthetic organic chemistry and medicinal chemistry as they represent substructures often encountered in numerous bioactive natural isolates and pharmaceutically important compounds.[1] Some illustrative examples are depicted in Fig. 1 including (+)-oleracein,[1b] (−)-trolline,[1c] (+)-crispine[1d] and lamellarin alkaloids such as lamellarin D and lamellarin α-20-sulfate.[1f] Most of the pyrrolo[2,1-*a*]isoquinoline alkaloids display remarkable antitumor,[2] antibacterial and antiviral,[3] anti-inflammatory,[4] antidepressant[5] and cardiovascular[6] properties. Furthermore, lamellarin D, isolated from marine molluscs, has been reported to be an inhibitor of human topoisomerase,[7] whereas lamellarin α-20-sulfate inhibits the enzyme HIV integrase.[1e,8] Owing to the intriguing synthetic value and multiple biological activities of these heterocyclic systems, development of efficient and versatile synthetic methods allowing the construction of such scaffolds was strongly encouraged.

In the past decade, 1,3-dipolar cycloaddition reactions of isoquinolinium *N*-ylides with activated alkynes or olefins[9] have arguably emerged as a fascinating and powerful tool for the synthesis of pyrrolo[2,1-*a*]isoquinoline derivatives. However, a survey of the literature reveals that the reported 1,3-dipoles were generated *in situ* by basic deprotonation of their

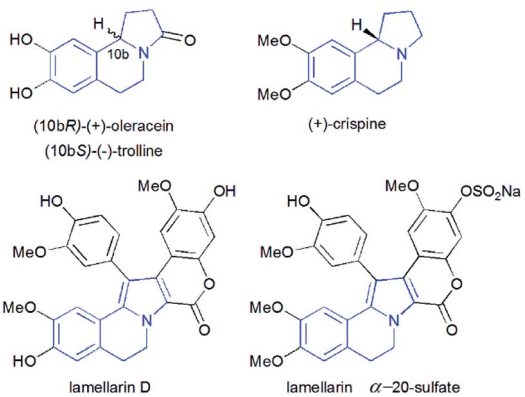

Fig. 1 Structures of some pyrrolo[2,1-*a*]isoquinoline alkaloids.

[a]*Laboratory of Heterocyclic Chemistry Natural Product and Reactivity/CHPNR, Department of Chemistry, Faculty of Science of Monastir, 5000 Monastir, Tunisia. E-mail: sarra_boudriga@yahoo.fr*

[b]*Departement of Chemistry, Quebec Center for Functional Materials University of Sherbrooke, Sherbrooke, Quebec, Canada J1K 2R1*

[c]*Institut UTINAM - UMR CNRS 6213, Université Bourgogne Franche-Comté, 16 Route de Gray, 25030 Besançon, France*

[d]*Technische Universität Dortmund, Anorganische Chemie, Otto-Hahn-Strasse 6, 44221 Dortmund, Germany*

† Electronic supplementary information (ESI) available. CCDC 1585506, 1585512 and 1585515. For ESI and crystallographic data in CIF or other electronic format see DOI: 10.1039/c8ra09884k

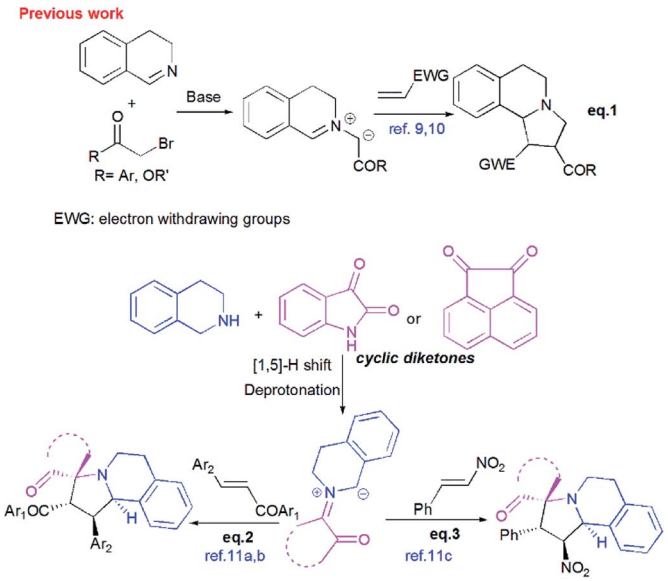

Scheme 1 Strategy for direct construction of spiropyrrolo[2,1-*a*]isoquinoline derivatives.

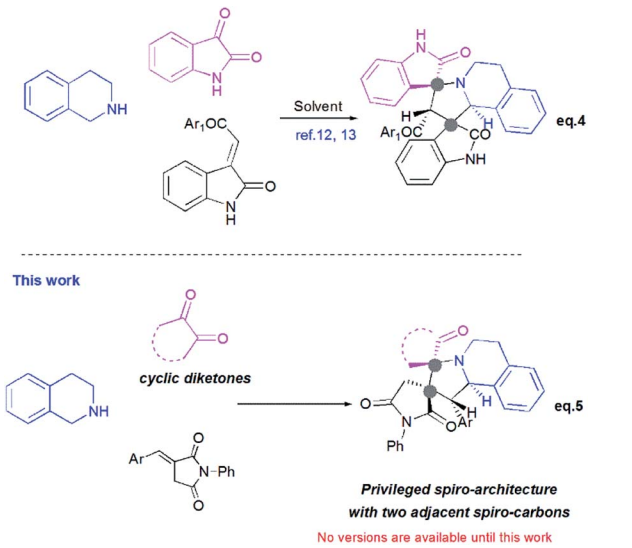

Scheme 2 Profile of 1,3-dipolar cycloaddition for exocyclic enones with tetrahydroisoquinolinium *N*-ylides derived from cyclic diketones.

corresponding isoquinolinium bromides (Scheme 1, eqn (1)).[9,10] These latter were prepared mainly by the condensation of isoquinoline with substituted phenacyl bromide or alkylbromoacetates.

However, tetrahydroisoquinolinium *N*-ylide stemming from cyclic diketones have rarely been considered as azomethine ylide precursors.

So far, Sarrafi *et al.*[11] developed the first examples of multicomponent 1,3-dipolar cycloaddition reaction involving acenaphthenequinone and isatin as cyclic diketones-based tetrahydroisoquinolinium *N*-ylides with chalcone and nitrostyrene derivatives as dipolarophiles (Scheme 1, eqn 2 and 3).[11] The azomethine ylides were produced *in situ via* [1,5]-H shift and subsequent deprotonation.

Recently, Huang[12] and Kumar[13] successfully developed a [3+2]-cycloaddition reaction of 2-oxoindolin-3-ylidene derivatives with azomethine ylides derived from isatin and 1,2,3,4-tetrahydroisoquinoline, and only one single regioisomer, namely dispiroindoline-3,1′-pyrrolo[2,1-*a*]isoquinoline-3′,3′-indoline-2,2″-dione was obtained. Generally, it has been found that dispiropyrrolo[2,1-*a*]isoquinoline derivatives were selectively formed in this kind of 1,3-dipolar cycloadditions. However, the alternative regioisomer incorporating two adjacent spiro-carbons, has never been reported (Scheme 2, eqn (4)).[12–14] In spite of this initial work, the systematic investigation on 1,3-dipolar cycloaddition involving exocyclic enones and tetrahydroisoquinolinium *N*-ylides derived from cyclic diketones is still rather limited and represents certainly interesting opportunities for further development.

New advances in this area could afford a convenient approach to structurally novel pyrrolo[2,1-*a*]isoquinoline derivatives bearing multiple neighboured stereogenic centres, which may provide some benefits to medicinal chemistry and drug discovery. Considering this challenge, we wondered whether α-alkylidenesuccinimides could be employed as exocyclic enones to undergo [3+2] cycloaddition using tetrahydroisoquinolinium *N*-ylides derived from cyclic diketones, thus yielding dispiropyrrolo[2,1-*a*]isoquinoline derivatives.

On the other hand, our targeted formal 1,3-dipolar cycloaddition products contain pyrrolidinone-2,5-dione scaffolds. These latter have the important advantage of being present in a great variety of natural products as well as in a vast library of synthetic compounds endowed with several bioactivities.[15] Recently, we reported the synthesis of functionalized spirooxindolepyrrolidines and dispiropyrrolothiazoles containing the pyrrolidine-2,5-dione motif which exhibits antibacterial, antifungal, antimalarial, and antimycobacterial activities.[16]

Herein, and in continuation of our research in the area of [3+2] cycloaddition of azomethine ylides,[16,17] we describe for the first time the formation of the hitherto unknown regioisomer, with two adjacent spiro-carbons, by 1,3-dipolar cycloaddition reactions of cyclic diketones-based tetrahydroisoquinolinium *N*-ylides and α-alkylidenesuccinimides. This route provides an attractive access to novel dispiropyrrolo[2,1-*a*]isoquinolines with a broad substrate scope in good to high yields. The stereochemistry of the spiroadducts has been confirmed by three X-ray diffraction studies. Moreover, to better rationalize mechanistically this kind of reaction, the regio- and stereochemistry of dispiropyrrolo[2,1-*a*]isoquinoline was investigated by means of Density Functional Theory (DFT) calculations.

Results and discussion

Three-component synthesis of the spiropyrrolo[2,1-*a*] isoquinolines

At the onset of our work, (*E*)-3-benzylidene-1-phenylpyrrolidine-2,5-dione **1a**, isatin **2a** and 1,2,3,4-tetrahydroisoquinoline (THIQ) **3** were employed as substrate models to optimize the reaction conditions (Scheme 3, Table 1). The reaction was

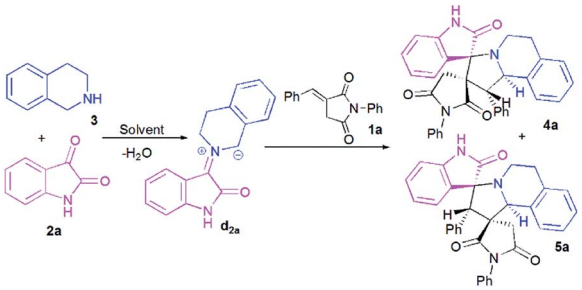

Scheme 3 Reaction of (*E*)-3-benzylidene-1-phenylpyrrolidine-2,5-dione **1a** with isatin **2a** and 1,2,3,4-tetrahydroisoquinoline (THIQ) **3**.

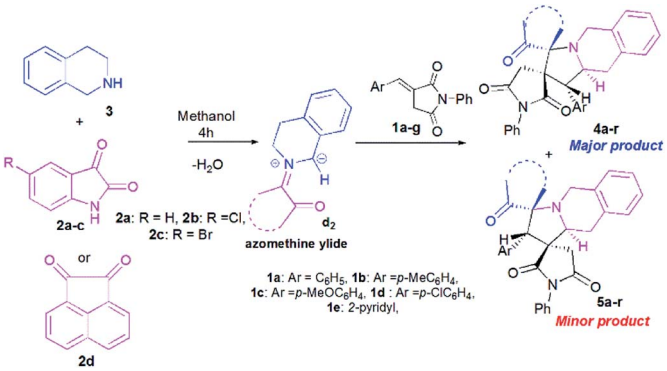

Scheme 4 Reaction of (*E*)-3-arylidene-1-phenylpyrrolidine-2,5-dione **1a–g** with cyclic diketones **2** and 1,2,3,4-tetrahydroisoquinoline (THIQ) **3**.

Table 1 Optimization of the 1,3-dipolar cycloaddition of dipolarophile **1a** with isatin **2a** and 1,2,3,4-tetrahydroisoquinoline (THIQ) **3a**[a]

Entry	Solvent	*T* (°C)	Time (h)	rr[c] (4 : 5)	Yield[d] (%)
1	$PhCH_3$	25	24	—	NR[b]
2	MeOH	25	24	—	NR[b]
3	EtOH	25	24	—	NR[b]
4	CH_3CN	25	24	—	NR[b]
5	$PhCH_3$	Reflux	12	—	Trace
6	CH_3CN	Reflux	6	52 : 48	55
7	EtOH	Reflux	4	60 : 40	65
8	**MeOH**	**Reflux**	**4**	**60 : 40**	**85**

[a] The reaction was carried out in 0.2 mmol scale in solvent (2 mL), and the ratio of **1a**/**2a**/**3** is 1 : 1 : 1.2. [b] No reaction due to insufficient solubility. [c] The regioisomeric ratio (rr) was determined by ^{1}H NMR spectra of the crude reaction mixture. [d] Combined yield of isolated **4a** and **5a**.

investigated with different solvents of different polarities such as methanol, ethanol, acetonitrile and toluene.

As shown in Table 1, the reaction does not proceed at room temperature (Table 1, entries 1–4) and does not occur in refluxing toluene (Table 1, entry 5). Surprisingly, in acetonitrile, the reaction proceeds smoothly affording the corresponding spiropyrrolo[2,1-*a*]isoquinolines as a mixture of two regioisomers **4a** and **5a** in a 60 : 40 ratio, albeit with a moderate yield (Table 1, entry 6). As can be seen from Table 1, the best results were obtained by refluxing the reaction mixture in methanol for 4 h, providing isomeric dispiropyrrolo[2,1-*a*]isoquinolineoxindoles **4a** and **5a** in high yield (85%), along with high diastereoselectivities (Table 1, entry 8).

Once the optimal conditions being established (Table 1, entry 8), we tried to extend the scope of this reaction with different *p*-aryl substituted dipolarophiles **1**, as well as with various diketones **2a–d** (Scheme 4, Table 2). The electronic properties exerted by the substituent at the *p*-position of the aryl group of imides **1** were shown to have little influence on the efficiency of this reaction (Table 2). For example, enones **1** bearing an electron-neutral (H), or electron-donating (*e.g.*, 4-Me or 4-OMe) group or electron-withdrawing substituent (Cl) or group (2-pyridinyl) reacted smoothly to give isomeric spiropyrrolo[2,1-*a*]isoquinolineoxindoles products in excellent yields (Table 2, entries 1–5).

However, the regioselectivity of these reactions was quite poor. Moreover, it seems that the electronic effects induced by (i) halogen substituents (Cl and Br) on the phenyl ring of isatin (Table 2, entries 6–13) or (ii) acenaphthenequinone **2d**, as cyclic diketone (Table 2, entries 14–18), were beneficial for increasing the regioselectivities. All compounds were isolated as colourless solids.

Spectroscopic and crystallographic characterization of the isomeric cycloadducts

The structure and the relative configuration of the isomeric pyrrolo[2,1-*a*]isoquinolines resulting from the cycloaddition were deduced from NMR in solution and, in the solid state from X-ray structure determinations performed on cycloadducts **4a**, **5a** and **5r**.

Table 2 Synthesis of the dispiropyrrolo[2,1-*a*]isoquinolines **4** and **5**[a]

Entry	Comp.	Diketone	Ar	rr[b] (4 : 5)	Yield[d] (%)
1	**4a** + **5a**	**2a**	C_6H_5	60 : 40[c]	85
2	**4b** + **5b**	**2a**	*p*-MeC_6H_4	65 : 35	88
3	**4c** + **5c**	**2a**	*p*-$MeOC_6H_4$	68 : 32[c]	87
4	**4d** + **5d**	**2a**	*p*-ClC_6H_4	68 : 32[c]	80
5	**4e** + **5e**	**2a**	2-Pyridyl	60 : 40	82[e]
6	**4f** + **5f**	**2b**	C_6H_5	80 : 20	85
7	**4g** + **5g**	**2b**	*p*-MeC_6H_4	83 : 17	83
8	**4h** + **5h**	**2b**	*p*-$MeOC_6H_4$	>90 : 10	87[e]
9	**4i** + **5i**	**2b**	2-Pyridyl	>90 : 10	85[e]
10	**4j** + **5j**	**2c**	C_6H_5	>90 : 10	80[e]
11	**4k** + **5k**	**2c**	*p*-MeC_6H_4	85 : 15	88
12	**4l** + **5l**	**2c**	*p*-$MeOC_6H_4$	86 : 14	85
13	**4m** + **5m**	**2c**	2-Pyridyl	>90 : 10	83[e]
14	**4n** + **5n**	**2d**	C_6H_5	77 : 23	72
15	**4o** + **5o**	**2d**	*p*-MeC_6H_4	78 : 22[c]	75[f]
16	**4p** + **5p**	**2d**	*p*-$MeOC_6H_4$	78 : 22	67
17	**4q** + **5q**	**2d**	*p*-ClC_6H_4	90 : 10	63
18	**4r** + **5r**	**2d**	2-Pyridyl	80 : 20[c]	65[f]

[a] The reaction was carried out in 1 mmol scale in methanol (5 mL) at reflux for 4 h, and the ratio of **1**/**2**/**3** is 1 : 1 : 1.2. [b] Unless otherwise noted, the regioisomeric ratio (rr) was determined by the isolated yields of **4** and **5**. [c] Determined by ^{1}H NMR analysis of the crude product. [d] Combined yields of isolated **4** and **5**. [e] Failed to separate compound **5**. [f] Failed to separate compound **4**.

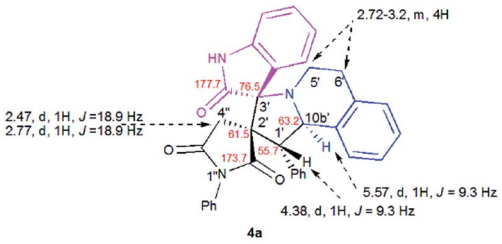

Fig. 2 Selected ^{1}H and ^{13}C NMR chemical shifts of **4a**.

Relevant ^{1}H and ^{13}C chemical shifts of pyrrolo[2,1-*a*]isoquinolines **4a** and **5a** are shown in Fig. 2 and 3, respectively. The ^{1}H NMR spectrum of **4a** shows two mutually coupled doublets at δ 2.47 and 2.77 ppm ($J = 18.9$ Hz) corresponding to the diastereotopic 4′-CH_2, as well as two further doublets at δ 4.38 ($J = 9.3$ Hz) and 5.57 ppm ($J = 9.3$ Hz) assigned to the pyrrolidine H-1′ and H-10b′ protons (Fig. 2), respectively.

Their coupling constants of approximately 9 Hz indicate that these protons are *trans*-arranged. The occurrence and the multiplicity of these signals clearly prove the regiochemistry of the cycloaddition reaction. In contrast, in the ^{1}H NMR spectrum of regioisomer **5a** (Fig. 3), the pyrrolidinyl protons H-2′ and H-10b′ appear as two singlets resonating at δ 4.64 and 5.74 ppm, respectively. The ^{13}C NMR spectra of all synthesized spirooxindoles exhibit two peaks atδ 74.1–76.5 and 177.7–179.2 ppm for the spiro-carbon and the oxindole carbonyl group, respectively.

The regio- and the stereochemical outcome of the cycloadditions were unambiguously ascertained by X-ray analysis of the crystal structure of cycloadducts **4a**, **5a** and **5r**, whose molecular structures are depicted in Fig. 4, 5 and 6, respectively. The crystal data collection and refinement data are summarized in Table 3.

Elucidation of the three structures reveals that (i) the two carbonyl carbons of the enone part and isatin or acenaphthenequinone moieties are in *trans*-relationship, and (ii) a *cis*-relationship between the carbonyl of the oxindole or acenaphthenequinone ring and the proton attached at C-10b′. Thus, the cycloadducts are formed through an *exo*-approach between the ***syn*-$\mathbf{d_2}$** and (*E*)-3-arylidene-1-phenyl-pyrrolidine-2,5-diones **1** (Scheme 4). The cycloaddition proceeds with high *exo*-diastereoselectivity affording in each case only one diastereomer. It is worth noting that our result is in contrast to the observed diastereoselectivity outcome from previously published studies.[11]

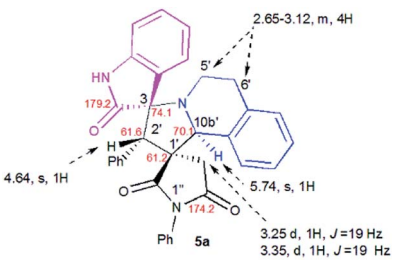

Fig. 3 Selected ^{1}H and ^{13}C NMR chemical shifts of **5a**.

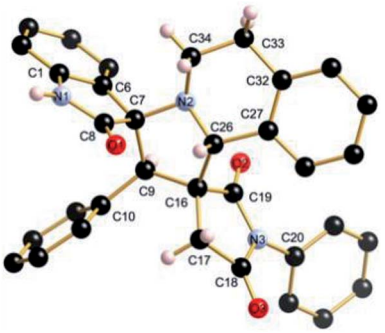

Fig. 4 Ball and sticks presentation of the molecular structure of **4a** in the crystal. For clarity, only stereochemically significant hydrogen atoms are shown. Selected bond lengths (Å) and angles (°): C4–N8 1.3991(16), C10–N8 1.3992(16), C10–O3 1.2015(17), C4–O1 1.2012(16), C19–N5 1.4506(18), C27–N5 1.4582(17), C15–N7 1.3441(18), C15–O2 1.2295(16); C4–N8–C10 112.14(11), C27–N5–C20 114.71(11), N5–C20–C36 105.63(12), C19–C16–C25 104.23(10), C25–C27–N5 101.17(10), C27–N5–C19 107.04(11), N5–C19–C15 111.46(11).

These works handled 1,3-dipolar cycloaddition reactions with tetrahydroisoquinolinium *N*-ylides derived from cyclic diketones. The authors revealed that the products were formed selectively through an *endo*-approach between *syn*-ylide and the dipolarophile.

DFT calculations

To better grasp the experimentally observed high diastereoselectivity in the multicomponent 1,3-dipolar cycloaddition, calculations using the density functional approach (DFT) were performed. The effect of solvent (methanol) was estimated using the polarizable continuum model (PCM) approach.

The model case study was the reaction of the dipolarophile **1a** with azomethine ylide $\mathbf{d_{2b}}$ formed from the condensation of THIQ with chloroisatin **2b** which should lead to the formation of the two types of iminium ions, *Z* and *E* (Scheme 5). For the generation of an azomethine ylide *via* a [1,5]-H shift, the oxygen

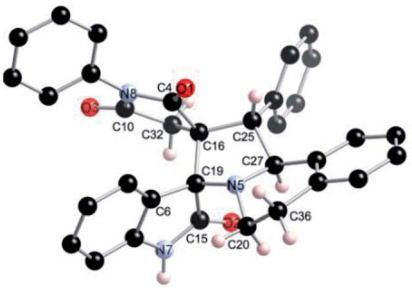

Fig. 5 Ball and sticks presentation of the molecular structure of **5a** in the crystal. For clarity, only stereochemically significant hydrogen atoms are shown. Selected bond lengths (Å) and angles (°): C8–O1 1.224(4), C8–N1 1.366(4), N1–C1 1.409(4), C19–O2 1.207(3), C19–N3 1.401(4), N3–C18 1.386(4), C18–O3 1.220(3), N2–C26 1.471(4), N2–C34 1.460(4); C1–N1–C8 112.2(3), C8–C7–N2 112.6(2), C7–N2–C34 116.9(2), C7–N2–C26 105.9(2), C16–C26–N2 103.0(2), C27–C26–N2 110.3(2), C19–N3–C18 112.3(2), N3–C18–C17 108.6(3), N3–C19–C16 108.8(2).

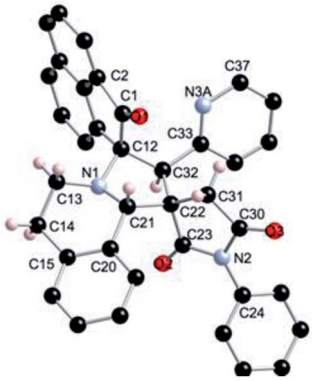

Fig. 6 Ball and sticks presentation of the molecular structure of **5r** in the crystal. For clarity, only stereochemically significant hydrogen atoms are shown. Selected bond lengths (Å) and angles (°): C1–O1 1.2134(17), C12–N1 1.4760(18), N1–C21 1.4577(17), C23–O2 1.2086(17), C23–N2 1.3935(17), N2–C30 1.3975(17), C30–O3 1.2107(16); C12–N1–C21 106.09(10), N1–C21–C22 103.57(11), C21–C22–C23 112.90(11), C32–C12–N1 98.54(10), C22–C23–N2 108.53(11), C23–N2–C30 112.73(11), N2–C30–C31 108.11(11), C31–C22–C32 115.82(11).

of the carbonyl group of the *E* form is spatially too far from the benzylic hydrogen, while in the *Z* form they are close enough to permit a H-shift.[18] So, one can expect that the ***syn*-$\mathbf{d_{2b}}$** *N*-ylide would be formed from the *Z*-iminium salt.

Moreover, and in accordance with our previous work,[16b,17b] the attack of the dipolarophile on ***syn*-$\mathbf{d_{2b}}$** would enforce the inward movement of THIQ ring to the cyclic diketones core, thus enhancing the steric hindrance between these later nuclei. In the case of ***anti*-$\mathbf{d_{2b}}$**, the 1,3-dipolar cycloaddition of the *N*-ylide would be favoured because no apparent steric hindrance would have evolved from the outward movement of the THIQ core.[14,15b] Therefore, only the *syn*-*N*-ylide forming azomethine ylide $\mathbf{d_{2b}}$ are considered in the subsequent calculations.

This *syn* intermediate could in principle react with the dipolarophile **1a** along four reactive channels related to two regioisomeric and two stereoisomeric approaches (Scheme 6). The cycloadducts were labelled **4f**, **4′f**, **5f**, **5′f** and their transition states (TS) ***exo*-TS1**, ***endo*-TS1**, ***exo*-TS2** and ***endo*-TS2** were energetically optimized and characterized under the same level of calculation by using the Berny analytical gradient method.[19] These TS, which are characterized by a saddle point with a single imaginary frequency, are depicted in Fig. 7. The differences between reactants and transition states in the Gibbs free energy (ΔG), enthalpy (ΔH), entropy (ΔS) and internal energy (ΔU), for the different stationary points along the reactive pathways are compiled in Table 4.

All the energy values have been corrected for the zero point energy. The kinetic parameters (activation energy $\Delta G^{\#}$,

Table 3 Crystal data collection and structure refinement of **4a**, **5a** and **5r**

Compound/formula	**4a**/$C_{34}H_{27}N_3O_3$	**5a**/$C_{34}H_{27}N_3O_3$	**5r**/$C_{37}H_{27}N_3O_3$
Formula weight	525.58	525.58	561.61
Temperature/K	150(2)	150(2)	150(2)
Wavelength/Å	0.71073	0.71073	0.71069
Crystal system	Triclinic	Orthorhombic	Monoclinic
Space group	$P\bar{1}$	$P2_12_12_1$	$P2_1/c$
a/Å	7.8139(9)	9.5047(6)	11.7916(5)
b/Å	12.9798(6)	11.4368(7)	9.7185(4)
c/Å	14.2280(7)	23.899(2)	24.5997(10)
α	65.084(5)°	90°	90°
β	80.892(11)°	90°	91.888(4)°
γ	79.404(3)°	90°	90°
Volume/Å^3	1281.12(11)	2598.0(3)	2817.5(2)
Z	2	4	4
Density (calculated) g cm^{-3}	1.362	1.344	1.324
Absorp. coefficient/mm^{-1}	0.088	0.087	0.085
F(000)	552.0	1104.0	1176
Crystal size/mm^3	0.10 × 0.10 × 0.41	0.19 × 0.11 × 0.07	0.30 × 0.20 × 0.10
Theta range for data collection/°	5.32 to 54.00	4.61 to 51.99	4.50 to 54.00
Index ranges	$-9 \le h \le 9$, $-16 \le k \le 16$ $-18 \le l \le 18$	$-10 \le h \le 11$ $-12 \le k \le 14$ $-26 \le l \le 29$	$-15 \le h \le 15$ $-13 \le k \le 13$ $-31 \le l \le 31$
Reflections collected	33 514	11 626	39 113
Independent reflections	5562 [R(int) = 0.0384]	5098 [R(int) = 0.0419]	6140 [R(int) = 0.0470]
Refinement method	Full-matrix least-squares on F^2	Full-matrix least-squares on F^2	Full-matrix least-squares on F^2
Data/restraints/parameters	5562/1/365	5098/1/365	6140/0/407
Goodness-of-fit on F^2	1.041	1.032	1.016
Final R indices [I > 2sigma(I)]	R_1 = 0.0423 wR_2 = 0.0973	R_1 = 0.0451 wR_2 = 0.0785	R_1 = 0.0440 wR_2 = 0.0934
R indices (all data)	R_1 = 0.0563, wR_2 = 0.1040	R_1 = 0.0679, wR_2 = 0.0875	R_1 = 0.0607, wR_2 = 0.1022
Largest diff. peak and hole/e Å^{-3}	0.31 and −0.24	0.18 and −0.24	0.26 and −0.24

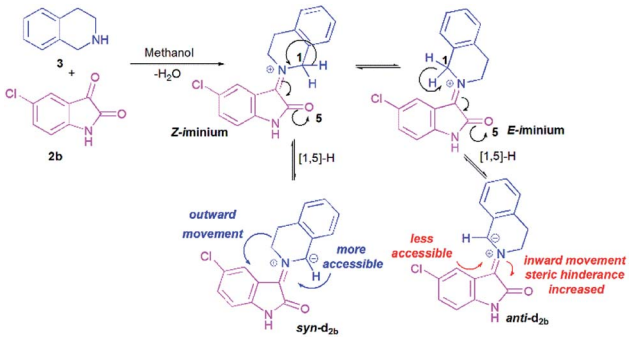

Scheme 5 Generation of azomethine ylide $\mathbf{d_{2b}}$.

activation enthalpies $\Delta H^{\#}$, and activation entropies $\Delta S^{\#}$ between reactants and TS) are first discussed.

The corresponding activation parameters, $\Delta H^{\#}$, $\Delta S^{\#}$ and $\Delta G^{\#}$, are in fairly good agreement with the experiment results. However, the strong negative entropy values of ***exo*-TS1** and ***exo*-TS2** suggest a highly ordered rate-determining transition state, as expected for a polar concerted cycloaddition.[20]

The potential energy requested to reach the TS, *i.e.*, the activation energy, was shown to increase in the following order: ***exo*-TS2** < ***exo*-TS1** < ***endo*-TS1** < ***endo*-TS2**.

The favoured *exo* approaches compared with the *endo* attack agree well with experimental findings showing that mixtures of the two *exo*-regioisomers are observed only.

The thermodynamic parameters, ΔG, ΔH and ΔS, between reactants and products of the investigated reactions are reported in Table 4.

The lowest ΔG value is achieved for the *exo* approach on **4f** (3.1 kcal mol^{-1}). In addition, cycloadditions leading to **4f**, **5f**, **4′f** and **5′f** are exothermic processes, and the most negative values of ΔH correspond to **4f** and **5f** (-10.6 and -8.7 kcal mol^{-1}, respectively). It is worth noting that calculations in methanol solution indicate positive free Gibbs energies ($\Delta G > 0$) for these reactions. Moreover, the cycloadduct **4f** resulting from the *exo* approach of ***syn*-$\mathbf{d_{2b}}$** with dipolarophile **1a** is the most favourable thermodynamic product. TSs ***exo*-TS1** and ***exo*-TS2** of the two cycloadducts **4f** and **5f** respectively, exhibit comparable energies. They are thus the two outcomes, but due to a clear difference in energy, **4f** is the major product.

All the TS are concerted asynchronous as expected for a typical normal-demand 1,3-dipolar cycloaddition. To support this accordance, the two new σ bonds lengths l_1 and l_2 are measured. At the TSs associated with the approach affording the cycloadducts **4f** and **4′f** (Fig. 7), the length of the C-1′–C-10b′ forming bonds are 1.991 Å at ***exo*-TS1** and 1.974 Å at ***endo*-TS1**, while the distance between the C-2′ and the C-3′ atoms is 2.469 Å at ***exo*-TS1** and 2.649 Å at ***endo*-TS1**. However, the opposite trend is found for fused transition structures (***exo*-TS2** and ***endo*-TS2**), with forming C-1′–C-3′ bond lengths of 1.996 Å and 2.001 Å, respectively. The computed distance between the C-2′ and the C-10b′ atoms is 2.490 Å at ***exo*-TS2** and 2.417 Å at ***endo*-TS2**.

The extent of the asynchronicity of the bond-formation can thus be measured by the difference between the lengths of the two σ bonds being formed in the reaction, *i.e.*, $\Delta d = l_1 - l_2$. The asynchronicity at the first trend leading **4f** and **4′f** is $\Delta d = 0.478$ Å at ***exo*-TS1** and 0.675 Å at ***endo*-TS1**, while that at the second tend affording **5f** and **5′f** is $\Delta d = 0.494$ Å at ***exo*-TS2** and 0.416 Å at ***endo*-TS2**. Therefore, the formation of the TSs associated with **4f** and **5f** is favoured. In addition, these geometrical parameters indicate that these cycloadditions correspond to asynchronous concerted processes.

Frontier molecular orbitals (FMO) have been determined in order to get global reactivity indices. These indices, namely, electronic chemical potential, μ, chemical hardness, η, and global electrophilicity, ω, are powerful tools for studying the feasibility of the reaction, as well as the reactivity of the reagents.[21] They have been computed for the separated reagents

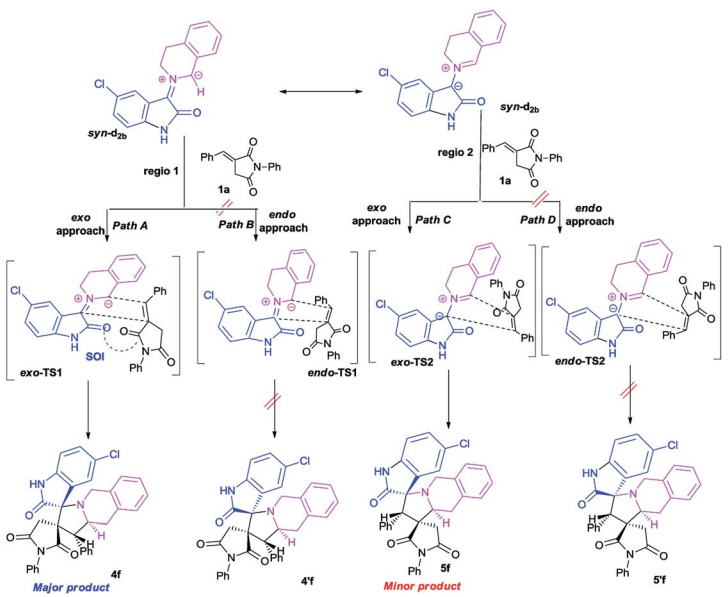

Scheme 6 Plausible mechanism for the regio- and stereoisomeric 1,3-dipolar cycloaddition reaction of dipolarophile **1a** with ***syn*-$\mathbf{d_{2b}}$**.

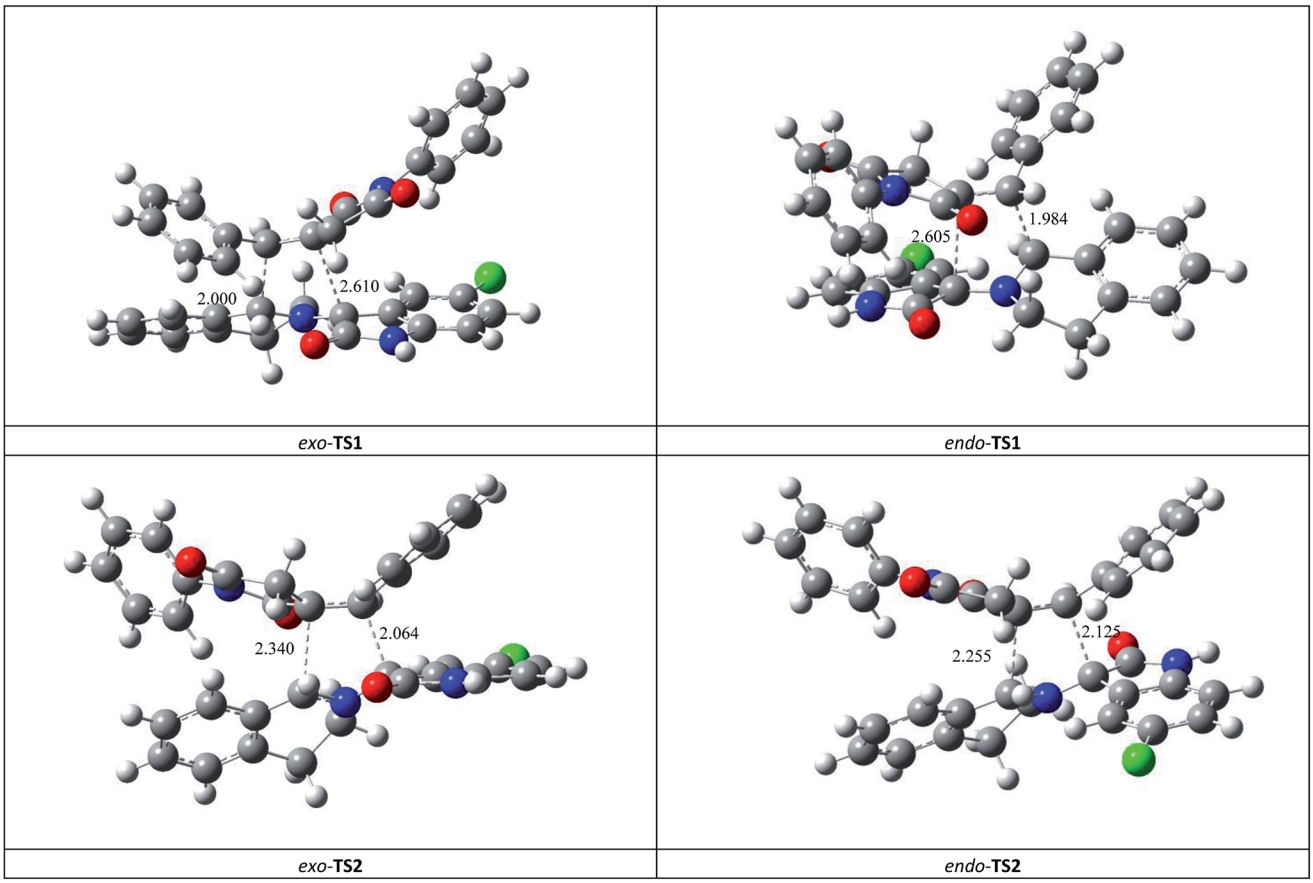

Fig. 7 Four possible TS for the 1,3-dipolar cycloaddition of ***syn*-$\mathbf{d_{2b}}$** across **1a**, optimized at the B3LYP/6-31G(d,p) level. The lengths of the bonds directly involved in the reaction are given in Å. Coordinates are given in the ESI.†

involved in the [3+2] cycloaddition reaction of dipolarophile **1a** with azomethineylide ***syn*-$\mathbf{d_{2b}}$**. The chemical hardness η reveals the stability and reactivity of a chemical system.[22–24] The global electrophilicity ω measures the propensity or capacity of a species to accept electrons.[24g,25] All the data are displayed in Table S1.†

Analysis of the reactive indices suggests that the electronic chemical potential μ of dipole ***syn*-$\mathbf{d_{2b}}$** (−3.921 eV) is higher than that of dipolarophile **1a** (−4.343 eV) and the chemical hardness of ***syn*-$\mathbf{d_{2b}}$** ($\eta = 3.624$ eV) is lower than of **1a** ($\eta = 4.595$ eV). This result indicates that the charge transfer will take place from the dipole toward dipolarophile. Over and above, the electrophilicity of dipolarophile **1a** ($\omega = 2.052$ eV) is greater than that of ***syn*-$\mathbf{d_{2b}}$** ($\omega = 2.237$ eV), indicating that the 1,3-dipole will act as a nucleophile due to its low ω value and high global nucleophilicity values ($N = 4.422$ eV). However, the dipole ***syn*-$\mathbf{d_{2b}}$** is classified as strong nucleophiles due to its high nucleophilicity index, $N > 3$ eV.[26] **1a** will thus act as an electrophile.

Table 4 Relative Gibbs free energies at 298.15 K (ΔG, in kcal mol^{-1}), enthalpies (ΔH, in kcal mol^{-1}) and entropies (ΔS, in cal mol^{-1} K^{-1}) for TSs and adducts of 1,3-dipolar cycloaddition between ***syn*-$\mathbf{d_{2b}}$** and **1a**, calculated at the B3LYP/6-31G(d,p) level

	ΔG	ΔH	ΔS	ΔU
4f	3.1	−10.6	−46.0	−13.7
4′f	6.6	−6.7	−44.8	−9.4
5f	6.7	−8.7	−51.6	−11.1
5′f	9.6	−5.4	−50.1	−7.7
***exo*-TS1**	23.8	9.5	−47.8	8.3
***endo*-TS1**	25.5	11.7	−46.1	10.7
***exo*-TS2**	23.1	9.3	−46.2	8.2
***endo*-TS2**	26.7	13.2	−45.3	12.1

After evaluation of the global nucleophilic/electrophilic character, a local analysis was carried out with the calculation of condensed Fukui functions considering the cationic and anionic systems in their optimized geometries of the corresponding neutral systems. Fukui function parameters have been evaluated through the calculation of the electrostatic potential (ESP) derived atomic populations.[27] The calculated local chemical reactivity parameters of ***syn*-$\mathbf{d_{2b}}$** and dipolarophile **1a** are shown in Fig. S1 (in the ESI).† We can notice that C-10b′ of azomethine ylide ***syn*-$\mathbf{d_2}$** has more nucleophilic character ($f^- = 0.162$). On the other hand, the dipolarophile **1a** has the highest electrophilic centre at C-1′ ($f^+ = 0.118$). The electrophilicity at C-1′ can be attributed to the presence of a strong electron-withdrawing carbonyl group. Thereby, the most favourable nucleophilic/electrophilic interaction will occur between C-10b′ carbon atom of ***syn*-$\mathbf{d_2}$** and C-1′ atom of enone

1a leading to preferred formation of major regioisomer **4f**. These results perfectly agree with the experimental observations (Scheme 5).

Conclusion

We have thus developed an efficient method for the synthesis of a novel class of dispiropyrrolo[2,1-*a*]isoquinolines fused pyrrolidine-2,5-dione bearing two adjacent spiro-carbons in good to high yields with high diastereoselectivity. Our strategy to prepare these cycloadducts involves three-component 1,3-dipolar cycloaddition reaction between cyclic diketones as tetrahydroisoquinolinium *N*-ylides precursors and α-alkylidene-succinimides as dipolarophiles. More importantly, these findings proved the versatile utility of this strategy for the synthesis of complex dispiroheteropolycyclic systems, which is of great importance for the development of medicinally active drugs.

An analysis based on theoretical calculations using the DFT approach, B3LYP/6-31G(d,p) reveals that the isomeric spirocycloadducts **4** and **5** are obtained through a 1,3-dipolar cycloaddition reaction *via* a high asynchronous mechanism with very low activation energies, when compared to the other possible reaction paths. This outcome is in agreement with the experimental observations.

Experimental

Apparatus and general information

NMR spectra were recorded with a Bruker-Spectrospin AC 300 spectrometer operating at 300 MHz for ^{1}H and 75 MHz for ^{13}C using tetramethylsilane as the internal standard (0.00 ppm) in $CDCl_3$ as solvent. The following abbreviations were used to explain the multiplicities: bs = broad singlet, s = singlet, d = doublet, m = multiplet.

Elemental analyses were performed on a Perkin Elmer 2400 Series II Elemental CHNS analyzer. Materials: thin-layer chromatography (TLC): TLC plates (Merck, silica gel 60 F_{254} 0.2 mm 200 × 200 nm); substances were detected using UV light at 254 nm.

Typical representative procedure for preparation of cycloadducts 4a–5a

A mixture of **1a** (2 63 mg, 1.0 mmol), isatin **2a** (147 mg, 1 mmol) and tetrahydroisoquinoline **3** (159.7 mg, 1.2 mmol) was refluxed in methanol (5 mL) for 4 h. After completion of the reaction (TLC), the solvent was removed under vacuum. The residue was chromatographed on silica gel employing ethyl acetate-cyclohexane (3 : 7 v/v) as eluent to obtain the pure products **4a** (0.26 g, 51%) and **5a** (0.17 g, 34%). Spectroscopic data and further experimental details for the all compound are presented in the ESI.†

DFT calculations

The geometric optimizations of all reactants, TS, and products were performed using the B3LYP functional and the 6-31G(d,p) basis set in the Gaussian 09 (ref. 27) environment, by using the Berny analytical gradient method.[28] The global electrophilicity index, ω, was calculated following the expression,[24,25] $\omega = (\mu^2/2\eta)$, where μ is the electronic chemical potential, $\mu = (E_{HOMO} + E_{LUMO})/2$, and η is the chemical hardness, $\eta = (E_{LUMO} - E_{HOMO})$. The Fukui condensed functions have been calculated from local populations found from single point calculations carried out on reduced, neutral, and oxidized forms with geometries optimized for neutral species. The most favourable attack site can also be disclosed by theoretical calculations. The actual DFT-based local chemical reactivity Fukui function parameters for nucleophilic (f_k^+) and electrophilic (f_k^-) attacks were calculated through the electrostatic potential (ESP) derived atomic populations.[26]

Characterizations have been performed under the same level of calculation. Vibrational analysis has been performed for all the stationary points. TS are characterized by a single negative imaginary frequency. For all TS structures, the intrinsic reaction coordinate[27] calculation, using the Hessian-based predictor–corrector method,[28] was performed to ascertain that each TS connected the expected reactants and products. Thermal corrections were computed from unscaled frequencies for a standard state of 298.15 K and 1 atm in methanol solution and within the harmonic approximation.

Crystal structure determinations

A suitable crystal of **4a**, **5a** and **5r** was selected and mounted on an Xcalibur, Sapphire3 diffractometer. The crystals were kept at 150(2) K during data collection. Using Olex2,[29] the structures were solved with the ShelXS[30] structure solution program using Direct Methods and refined with the XL[30] refinement package using Least Squares minimisation.

Conflicts of interest

There are no conflicts to declare.

Acknowledgements

The computational resources were provided by Calcul Quebec and Compute Canada, through the financial support of the Canadian Foundation for Innovation (CFI).

References

1 (*a*) E. Marco, W. Laine, C. Tardy, A. Lansiaux, M. Iwao, F. Ishibashi, C. Bailly and F. Gago, *J. Med. Chem.*, 2005, **48**, 3796–3807; (*b*) L. Xiang, D. Xing, W. Wang, R. Wang, Y. Ding and L. Du, *Phytochemistry*, 2005, **66**, 2595–2601; (*c*) R. F. Wang, X. W. Yang, C. M. Ma, S. Q. Cai, J. N. Li and S. Yukihiro, *Heterocycles*, 2004, **63**, 1443–1448; (*d*) Q. Zhang, G. Tu, Y. Zhao and T. Cheng, *Tetrahedron*, 2002, **58**, 6795–6798; (*e*) M. V. R. Reddy, M. R. Rao, D. Rhodes, M. S. T. Hansen, K. Rubins, F. D. Bushman, Y. Venkateswarlu and D. J. Faulkner, *J. Med. Chem.*, 1999, **42**, 1901–1907; (*f*) R. J. Andersen, D. J. Faulkner,

H. C. Heng, G. D. V. Duyne and J. Clardy, *J. Am. Chem. Soc.*, 1985, **107**, 5492–5495.

2 (*a*) K. Tangdenpaisal, R. Worayuthakarn, S. Karnkla, P. Ploypradith, P. Intachote, S. Sengsai, B. Saimanee, S. uchirawat and M. Chittchang, *Chem.–Asian J.*, 2015, **10**, 925–937; (*b*) A. Theppawong, P. Ploypradith, P. Chuawong, S. Ruchirawat and M. Chittchang, *Chem.–Asian J.*, 2015, **10**, 2631–2650; (*c*) F. Plisson, X. C. Huang, H. Zhang, Z. Khalil and R. J. Capon, *Chem.–Asian J.*, 2012, **7**, 1616–1623.

3 (*a*) B. Su, C. Cai, M. Deng, D. Liang, L. Wang and Q. Wang, *Bioorg. Med. Chem. Lett.*, 2014, **24**, 2881–2884; (*b*) R. F. Wang, X. W. Yang, C. M. Ma, S. Q. Cai, J. N. Li and Y. Shoyama, *Heterocycles*, 2004, **63**, 1443.

4 C. J. Cavallito and A. P. Gray, *Fr. Pat.* 2135297, 1973Chem. Abstr. 1973, 79, 96989.

5 B. E. Maryanoff, J. L. Vaught, R. P. Shank, D. F. McComsey, M. J. Costanzo and S. O. Nortey, *J. Med. Chem.*, 1990, **33**, 2793–2797.

6 B. E. Maryanoff, D. F. MeComsey, J. F. Gardocki, R. P. Shank, M. J. Constanzo, S. O. Nortey, C. R. Schneider and P. E. Setler, *J. Med. Chem.*, 1987, **30**, 1433–1454.

7 E. Marco, W. Laine, C. Tardy, A. Lansiaux, M. Iwao, F. Ishibashi, C. Bailly and F. Gago, *J. Med. Chem.*, 2005, **48**, 3796–3807.

8 A. Aubry, X.-S. Pan, L. M. Fisher, V. Jarlier and E. Cambau, *Antimicrob. Agents Chemother.*, 2004, **48**, 1281–1288.

9 (*a*) R.-G. Shi, J. Sun and C.-G. Yan, *ACS Omega*, 2017, **11**, 7820–7830; (*b*) J. Sun, G.-l. Shen, Y. Huang and C.-G. Yan, *Sci. Rep.*, 2017, **7**, 41024; (*c*) R. Liu, R.-G. Shi, J. Sun and C.-G. Yan, *Org. Chem. Front.*, 2017, **4**, 354–357; (*d*) X.-H. Wang and C.-G. Yan, *Synthesis*, 2014, **46**, 1059–1066; (*e*) J. An, Q.-Q. Yang, Q. Wang and W.-J. Xiao, *Tetrahedron Lett.*, 2013, **54**, 3834–3837; (*f*) F. Dumitrascu, E. Georgescu, F. Georgescu, M. M. Popa and D. Dumitrescu, *Molecules*, 2013, **18**, 2635–2645; (*g*) L. Wu, J. Sun and C.-G. Yan, *Org. Biomol. Chem.*, 2012, **10**, 9452–9463; (*h*) Y. Shang, L. Wang, X. He and M. Zhang, *RSC Adv.*, 2012, **2**, 7681–7688; (*i*) J. L. G. Ruano, A. Fraile, M. R. Martín, G. González, C. Fajardo and A. M. M-Castro, *J. Org. Chem.*, 2011, **76**, 3296–3305; (*j*) J. L. G. Ruano, A. Fraile, M. R. Martín, G. González, C. Fajardo and A. M. M. Castro, *J. Org. Chem.*, 2011, **76**, 3296–3305; (*k*) F. Dumitrascu, M. R. Caira, E. Georgescu, F. Georgescu, C. Draghici and M. M. Popa, *Heteroat. Chem.*, 2011, **22**, 723–729; (*l*) K. M. Dawood, E. A. Ragab and N. A. Khedr, *J. Chin. Chem. Soc.*, 2009, **56**, 1180–1185; (*m*) Y. Liu, H.-Y. Hu, Q.-J. Liu, H.-W. Hu and J.-H. Xu, *Tetrahedron*, 2007, **63**, 2024–2033; (*n*) W. Peng and S. Zhu, *J. Chem. Soc., Perkin Trans. 1*, 2001, 3204–3210.

10 (*a*) S. Mondal, A. Maity, R. Paira, M. Banerjee, Y. P. Bharitkar, A. Hazra, S. Banerjee and N. B. Mondal, *Tetrahedron Lett.*, 2012, **53**, 6288–6291; (*b*) J. An, Q.-Q. Yang, Q. Wang and W. Xiao, *Tetrahedron Lett.*, 2013, **54**, 3834–3837; (*c*) Y. Liu, H.-Y. Hu, Q.-J. Liu, H.-W. Hu and J.-H. Xu, *Tetrahedron*, 2007, **63**, 2024–2033; (*d*) F. Dumitrascu, E. Georgescu, F. Georgescu, M. M. Popa and D. Dumitrescu, *Molecules*, 2013, **18**, 2635–2645; (*e*) A. Fujiya, M. Tanaka, E. Yamaguchi, N. Tada and A. Itoh, *J. Org. Chem.*, 2016, **81**, 7262–7270; (*f*) H.-M. Huang, Y.-J. Li, Q. Ye, W.-B. Yu, L. Han, J.-H. Jia and J.-R. Gao, *J. Org. Chem.*, 2014, **79**, 1084–1092.

11 (*a*) Y. Sarrafi, M. Hamzehlouian, K. Alimohammadi and H. R. Khavasi, *Tetrahedron Lett.*, 2010, **51**, 4734–4737; (*b*) Y. Sarrafi, A. Asghari, M. Hamzehloueian, K. Alimohammadic and M. Sadatshahabia, *J. Braz. Chem. Soc.*, 2013, **24**(12), 1957–1963; (*c*) K. Alimohammadi, Y. Sarrafi and B. Rajab, *C. R. Chim.*, 2013, **17**, 156–163.

12 Y. Huang, Y. X. Huang, J. Sun and C. G. Yan, *RSC Adv.*, 2018, **8**, 23990–23995.

13 N. S. Kumar, M. S. Reddy, V. R. Bheeram, S. B. Mukkamala, L. R. Chowhan and L. C. Rao, *Environ. Chem. Lett.*, 2018, 1–10.

14 I. Fejes, M. Nyerges, A. Szollosy, G. Blasko and L. Toke, *Tetrahedron*, 2001, **57**, 1129–1137.

15 (*a*) A. Fredenhagen, S. Y. Tamura, P. T. M. Kenny, H. Komura, Y. Naya, K. Nakanishi, K. Nishiyama, M. Sugiura and H. Kita, *J. Am. Chem. Soc.*, 1987, **109**, 4409–4411; (*b*) M. Isaka, N. Rugseree, P. Maithip, P. Kongsaeree, S. Prabpai and Y. Thebtaranonth, *Tetrahedron*, 2005, **61**, 5577–5583; (*c*) T. Matviiuk, G. Morid, C. Lherbeta, F. Rodriguez, M. R. Pasca, M. Gorichko, B. Guidettia, Z. Voitenko and M. Baltasa, *Eur. J. Med. Chem.*, 2014, **71**, 46–52; (*d*) M. Z. Wróbel, A. Chodkowski, F. Herold, A. Gomółka, J. Kleps, A. P. Mazurek, F. Pluciński, A. Mazurek, G. Nowak, A. Siwek, K. Stachowicz, A. Slawinska, M. Wolak, B. Szewczyk, G. Satala, A. J. Bojarski and J. Turlo, *Eur. J. Med. Chem.*, 2013, **63**, 484–500.

16 (*a*) S. Haddad, S. Boudriga, T. N. Akhaja, J. P. Raval, F. Porzio, A. Soldera, M. Askri, M. Knorr, Y. Rousselin, M. M. Kubicki and D. Rajani, *New J. Chem.*, 2015, **39**, 520–528; (*b*) S. Haddad, S. Boudriga, F. Porzio, A. Soldera, M. Askri, D. Sriram, P. Yogeeswari, M. Knorr, Y. Rousselin and M. M. Kubicki, *RSC Adv.*, 2014, **4**, 59462–59471.

17 (*a*) C. Mhiri, S. Boudriga, M. Askri, M. Knorr, D. Sriram, P. Yogeeswari, F. Nana, K. Golz and C. Strohmanni, *Bioorg. Med. Chem. Lett.*, 2015, **25**, 4308–4313; (*b*) S. Haddad, S. Boudriga, F. Parzo, A. Soldera, M. Askri, M. Knorr, Y. Rousselin, M. M. Kubicki, K. Golz and C. Strohmann, *J. Org. Chem.*, 2015, **80**, 9064–9075; (*c*) C. Mhiri, F. Rouatbi, S. Boudriga, M. Askri, K. Ciamala, M. Knorr, K. Monnier-Jobé, A. Khatyr, Y. Rousselin and M. M. Kubicki, *Mediterr. J. Chem.*, 2015, **4**, 30–50; (*d*) F. Rouatbi, M. Askri, F. Nana, G. Kirsch, S. Sriram and P. Yogeeswari, *Tetrahedron Lett.*, 2015, **57**, 163–167.

18 (*a*) K. Alimohammadi, Y. Sarrafi, M. Tajbakhsh, S. Yeganegi and M. Hamzehloueian, *Tetrahedron*, 2011, **67**, 1589–1597; (*b*) P. J. Xia, Y. H. Sun, J. A. Xiao, Z. F. Zhou, S. S. Wen, Y. Xiong, G. C. Ou, X. Q. Chen and H. Yang, *J. Org. Chem.*, 2015, **80**, 11573–11579.

19 (*a*) M. Cossi, V. Barone, R. Cammi and J. Tomasi, *Chem. Phys. Lett.*, 1996, **255**, 327–335; (*b*) E. Cances, B. Mennucci and J. Tomasi, *J. Chem. Phys.*, 1997, **107**, 3032–3041; (*c*) V. Barone, M. Cossi and J. Tomasi, *J. Comput. Chem.*, 1998, **19**, 404–417.

20 (*a*) R. Huisgen, 1,3-Dipolar Cycloadditions—Introduction, Survey, Mechanism, in *1,3-Dipolar Cycloaddition Chemistry*, ed. A. Padwa, John Wiley & Sons, Inc., New York, 1984, vol. 1, pp. 1–176; (*b*) K. N. Houk and K. Yamaguchi, Theory of 1,3-Dipolar Cycloadditions, in *1,3-Dipolar Cycloaddition Chemistry*, ed. A. Padwa, John Wiley & Sons, New York, 1984, vol. 2, pp. 407–447.

21 L. R. Domingo and J. A. Saez, *Org. Biomol. Chem.*, 2009, **7**, 3576–3583.

22 (*a*) A. V. Londhe, B. Gupta, S. Kohli, P. Pardasani and R. T. Z. Pardasani, *Z. Naturforsch., B: J. Chem. Sci.*, 2006, **61**, 213–220; (*b*) R. T. Pardasani, P. Pardasani, A. Jain and K. Arora, *Indian J. Chem.*, 2006, **45B**, 1204–1209; (*c*) K. Arora, D. Jose, D. Singh, R. S. Gupta, P. Pardasaniand and R. T. Pardasani, *Heteroat. Chem.*, 2009, **20**, 379–392.

23 (*a*) K. N. Houk, *Acc. Chem. Res.*, 1975, **8**, 361–369; (*b*) K. N. Houk, J. Sims, R. E. Duke, R. W. Strozier and J. K. George, *J. Am. Chem. Soc.*, 1973, **95**, 7287–7301; (*c*) K. N. Houk, J. Sims, C. R. Watts and L. J. Luskus, *J. Am. Chem. Soc.*, 1973, **95**, 7301–7315.

24 (*a*) R. G. Pearson, *Hard and soft acids and bases*, Dowden, Hutchinson, and Ross, Stroudsburg, PA, 1973; (*b*) R. G. Pearson, *Acc. Chem. Res.*, 1993, **26**, 250–255; (*c*) R. G. Pearson, *Chemical hardness: application from molecules to solid*, Wiley-VCH, Weinheim, 1997; (*d*) K. D. Sen and D. M. P. Mingos, *Chemical hardness: structure and bonding*, Springer, Berlin, 1993; (*e*) R. G. Parr and W. Yang, *Density functional theory of atoms and molecules*, Oxford University Press, New York, 1989; (*f*) P. G. Parr and R. G. Pearson, *J. Am. Chem. Soc.*, 1983, **105**, 7512–7516; (*g*) A. Vektariene, G. Vektaris and J. Svoboda, *ARKIVOC*, 2009, **7**, 311–329.

25 R. G. Parr, L. Szentpaly and S. Liu, *J. Am. Chem. Soc.*, 1999, **121**, 1922–1924.

26 (*a*) W. Yang and R. G. Parr, Hardness, softness, and the Fukui function in the electronic theory of metals and catalysis, *Proc. Natl. Acad. Sci. U. S. A.*, 1985, **82**, 6723; (*b*) S. Arulmozhiraja and P. Kolandaivel, *Mol. Phys.*, 1997, **90**, 55–62; (*c*) P. W. Ayers, W. Yang and L. Bartolotti, *Chemical Reactivity Theory: A Density Functional*, ed. P. K. Chattaraj, CRC Press, Boca Raton, FL, 2009, ch. 18.

27 (*a*) W. J. Hehre, L. Radom, P. v. R. Schleyer and J. A. Pople, *Ab initio Molecular Orbital Theory*, Wiley, New York, 1986; (*b*) K. Fukui, *J. Phys. Chem.*, 1970, **74**, 4161–4163.

28 (*a*) H. P. Hratchian and H. B Schlegel, *J. Chem. Theory Comput.*, 2005, **1**, 61–69; (*b*) V. Barone, M. Cossi and J. J. Tomasi, *Comput. Chem.*, 1998, **19**, 404–417.

29 O. V. Dolomanov, L. J. Bourhis, R. J. Gildea, J. A. K. Howard and H. Puschmann, *J. Appl. Crystallogr.*, 2009, **42**, 339–341.

30 (*a*) G. M. Sheldrick, *Acta Crystallogr.*, 2008, **A64**, 112–122; (*b*) G. M. Sheldrick, *Acta Crystallogr.*, 2015, **A71**, 3–8.